25p

NASA TN D-1617

N63-13188
Code 1

TECHNICAL NOTE

D-1617

A STUDY OF THE EFFECTS OF BANK ANGLE, BANKING DURATION, AND TRAJECTORY POSITION OF INITIAL BANKING ON THE LATERAL AND LONGITUDINAL RANGES OF A HYPERSONIC GLOBAL REENTRY VEHICLE

By Gene W. Sparrow

Langley Research Center
Langley Station, Hampton, Va.

NATIONAL AERONAUTICS AND SPACE ADMINISTRATION
WASHINGTON
March 1963

Copy 1

Code 1

NATIONAL AERONAUTICS AND SPACE ADMINISTRATION

TECHNICAL NOTE D-1617

A STUDY OF THE EFFECTS OF BANK ANGLE, BANKING DURATION, AND TRAJECTORY POSITION OF INITIAL BANKING ON THE LATERAL AND LONGITUDINAL RANGES OF A HYPERSONIC GLOBAL REENTRY VEHICLE

By Gene W. Sparrow

SUMMARY

An investigation has been made to determine the effect of banking position, bank angle, and banking duration on the lateral and longitudinal ranges of a hypersonic lifting reentry vehicle of global-range capability entering the atmosphere of a rotating oblate earth. Two schemes for controlling the angle of attack are used. Results indicate that banking the vehicle during the first half of a global-range reentry results in relatively large losses of longitudinal range without any appreciable gain in lateral range. In addition, it is found that lateral range can be obtained with less loss of longitudinal range if the scheme of using a small bank angle and an extended banking duration are used. A lift scheme which allows the angle of attack to increase during banking so that the vertical lift force does not decrease is not found to be as satisfactory as the constant angle-of-attack lift scheme because of relatively large losses of longitudinal range and reduced lateral-range capability.

INTRODUCTION

The ability of a reentry glider entering the earth's atmosphere to reach a given destination will depend upon adequate control of both lateral and longitudinal ranges. (See, for example, ref. 1.) Of paramount importance to the design of a range-control system for a reentry glider is the knowledge of the effect of a banking maneuver to obtain lateral range on the lateral and longitudinal ranges of the vehicle.

In the present paper the problem of obtaining lateral range is examined for the case of a reentry glider of global-range capability entering the atmosphere of a rotating oblate earth at near orbital speed and zero flight-path angle. Considered in the investigation are the effects of banking at various trajectory positions, of bank angle, and banking duration on the lateral and longitudinal ranges of the reentry glider. Results of this investigation were obtained by the utilization of a high-speed digital computer.

SYMBOLS

a	acceleration, ft/sec^2
$a_{x,a}, a_{y,a}, a_{z,a}$	acceleration components of lift and drag forces acting in the x, y, z directions, ft/sec^2
$a_{x,ob}, a_{y,ob}, a_{z,ob}$	acceleration components of oblateness forces acting in the x, y, z directions, ft/sec^2
C_D	drag-force coefficient
$C_{D,m}$	drag-coefficient parameter (m = 0, 1, 2)
C_L	lift-force coefficient
$C_{L,m}$	lift-coefficient parameter (m = 0, 1, 2)
D	drag force, lb
g_e	acceleration of gravity, ft/sec^2
h	altitude above surface of earth as measured from equator, ft
h_e	altitude above surface of earth, ft
$\bar{i}_s, \bar{j}_s, \bar{k}_s$	unit vectors in the x_s, y_s, z_s directions, respectively
K	trajectory banking position (position on trajectory where banking is initiated), deg
L	lift force, lb
$(L/D)_{max}$	maximum value of lift-drag ratio
m	mass of vehicle, slugs
M	Mach number
q	dynamic pressure, lb/sq ft
r_e	equatorial radius of earth, ft or nautical miles
$r_i, \eta_i, L_{c,i}$	spherical coordinates of X_i, Y_i, Z_i axes system
$r_r, \eta_r, L_{c,r}$	spherical coordinates of X_r, Y_r, Z_r axes system
R_{lat}	lateral range of vehicle, nautical miles

R_{long}	longitudinal range of vehicle, nautical miles
S	wing area, sq ft
t	time, sec unless otherwise indicated
V	velocity, ft/sec
V_e	magnitude of the vehicle velocity with respect to the earth, ft/sec
V_i	magnitude of the vehicle inertial velocity, ft/sec
X,Y,Z	moving axes with origin at center of mass of vehicle; Z axis is positive toward earth's geographical center and X axis is positive in the direction of increasing $L_{c,i}$
x,y,z	coordinates in X, Y, Z system
X_i,Y_i,Z_i	basic inertial axes (fixed in space); X_iY_i plane lies in equatorial plane of earth
x_i,y_i,z_i	coordinates in X_i, Y_i, Z_i system
X_r,Y_r,Z_r	secondary inertial axes (fixed in space); obtained from X_i, Y_i, Z_i axes by angular displacement σ about the X_i axis of basic inertial system
x_r,y_r,z_r	coordinates in X_r, Y_r, Z_r system
X_s,Y_s,Z_s	stability axes with origin at center of mass of vehicle orientated with respect to X, Y, Z axes by the usual Euler angle sequence of ψ, θ, and ϕ; X_s axis in the direction of the relative wind
x_s,y_s,z_s	coordinates in X_s, Y_s, Z_s system
α	angle of attack, radians or deg
ΔK	banking interval, deg
ΔR_{lat}	effective lateral range or difference in lateral ranges of banked and unbanked vehicle at termination of trajectory, nautical miles
ΔR_{long}	longitudinal range change or difference in longitudinal ranges of banked and unbanked vehicle at termination of trajectory, nautical miles

λ	earth longitude, radians or deg
μ	gravitational constant
ρ	atmospheric density, slug/cu ft
σ	inclination angle of reference plane to earth's equator
ψ,θ,ϕ	Euler angles used to orient stability axes with respect to XYZ moving axes system
ψ_i	inertial heading angle; angle measured in a clockwise direction from the X axis to the projection of V_i on the XY plane
ω	angular velocity of earth, radians/sec

Subscript:

0	value of variable at zero time

Dots above quantity denote differentiation with respect to time. All angles are in radians unless otherwise noted. A bar over a symbol indicates a vector.

ANALYSIS

Range of Investigation

The principal object of the present investigation is to determine the effect of trajectory banking position, bank angle, and duration of banking on the lateral and longitudinal ranges of the reentry vehicle. Two lift schemes which controlled the angle of attack of the vehicle during entry are used. In the basic lift scheme a constant angle of attack of 25° was maintained during the vehicle's descent. An optional lift scheme that was used to a limited extent allowed the angle of attack to increase from 25° during the banking phase of the descent so that the vertical lift force would not decrease because of banking. An extensive range of trajectory banking positions, bank angle, and durations of banking (subsequently referred to as banking interval) were used in the investigation.

Mathematical Model

Axes systems.- The axes systems employed in this investigation to define the motion and to measure ranges of the vehicle are presented in figure 1. The primary X_i, Y_i, and Z_i inertial axes are fixed in space with the X_iY_i plane being coincidental with the equatorial plane of the earth. The position of the vehicle was defined by the spherical coordinates $(r_i, \eta_i, L_{c,i})$ of the inertial-axes system. The equations of motion of the vehicle are written with respect to

the moving X, Y, and Z axes system with the center of mass of the vehicle at the origin of the axes system. The X, Y, and Z axes were pointed in the respective directions of increasing $L_{c,i}$, decreasing η_i, and decreasing r_i. The equations of motion of the vehicle are presented in appendix A.

The X, Y, and Z axes are orientated with respect to the X_s, Y_s, and Z_s stability axes by the usual Euler angle sequence of ψ, θ, and ϕ as shown in figure 1(b). The aerodynamic lift and drag forces of the vehicle with respect to the stability axes are:

$$\left.\begin{aligned} \bar{L} &= -L\bar{k}_s \\ \bar{D} &= -D\bar{i}_s \end{aligned}\right\} \tag{1}$$

where $\bar{k}_s$ and $\bar{i}_s$ are unit vectors in the direction of the Z_s and X_s axes, respectively. The transformation equations relating the X, Y, and Z axes and X_s, Y_s, and Z_s axes are presented in appendix A.

A secondary system of inertial axes X_r, Y_r, and Z_r containing the plane X_rY_r of the unperturbed reentry trajectory of the vehicle is used in measuring the lateral and longitudinal ranges of the vehicle, which are expressed as simple functions of the spherical coordinates $(r_r, \eta_r, L_{c,r})$ of the X_r, Y_r, and Z_r axes system. The reentry trajectory plane, subsequently referred to as the reference plane, is assumed to be inclined to the earth's equatorial plane (X_iY_i plane) by the angle $\sigma = 40^\circ$, with the line of nodes being chosen coincidental with the X_i axes.

Range measurements.- The lateral and longitudinal ranges of the vehicle are measured with respect to the reference plane X_rY_r with lateral range measured perpendicular to it and longitudinal range measured along the plane. The lateral and longitudinal ranges of the vehicle are defined as

$$\left.\begin{aligned} R_{lat} &= -r_e\left(\frac{\pi}{2} - L_{c,r}\right) \\ R_{long} &= r_e\eta_r \end{aligned}\right\} \tag{2}$$

where $L_{c,r}$ and η_r are angular spherical coordinates in the X_r, Y_r, and Z_r axes system, and r_e is the earth equatorial radius. The coordinates $L_{c,r}$ and η_r are generated from the coordinates $L_{c,i}$ and η_i by the conversion equations derived in appendix B.

The effect of banking the vehicle is measured by the corresponding changes in lateral and longitudinal ranges of the vehicle at h = 100,000 feet, when

compared to the trajectory of the unbanked vehicle and is defined by the range equations

$$\left.\begin{aligned} \Delta R_{lat} &= R_{lat} - 85.5 \\ \Delta R_{long} &= R_{long} - 23{,}581 \end{aligned}\right\} \tag{3}$$

where 85.5 and 23,581 are, respectively, the lateral and longitudinal ranges of the trajectory of the unbanked vehicle measured in nautical miles. The presence of lateral range in the trajectory of the unbanked vehicle is attributed to forces acting normal to the reference plane arising from an oblate rotating earth. The range-measurement scheme of equations (3) is illustrated graphically in figure 2 for the unbanked-vehicle trajectory and for a typical trajectory where banking was present. Lateral range is plotted against longitudinal range with the final portions of each trajectory shown.

Vehicle and earth model.- The reentry vehicle is represented by a point mass of 310 slugs and a wing area of 400 square feet with lift- and drag-force coefficients (table I) corresponding to a glider vehicle which has an $(L/D)_{max}$ capability of 2. Heading-angle changes of the vehicle were accomplished in the usual manner of banking an aircraft.

For the present analysis a rotating oblate-earth model is used and the atmosphere is assumed to rotate with the earth with density varying in altitude in accordance with the 1959 ARDC model atmosphere given in reference 2. The earth constants used in the investigation are as follows:

$$\mu = 0.273 \times 10^{-3}$$

$$\omega = 7.2722 \times 10^{-5} \text{ radians/sec}$$

$$r_e = 20{,}926{,}400 \text{ ft}$$

$$g_e = 32.147 \text{ ft/sec}^2$$

Initial Conditions

The initial conditions of the vehicle were chosen so that the earth longitude of the vehicle would change by 360° when the vehicle descended unbanked to an altitude of 100,000 feet and the vehicle would thus have global-range capability. The initial conditions used are the following:

$$h_0 = 390{,}800 \text{ ft}$$

$$\eta_{i,0} = 0^\circ$$

$$L_{c,i} = 90^\circ$$

$$\theta = 0^\circ$$

$$\psi_{i,0} = 230^\circ$$

$$V_{i,0} = 25{,}680 \text{ ft/sec}$$

Figure 3 shows the reentry trajectory of the unbanked vehicle for these initial conditions. The variation of altitude, velocity, and dynamic pressure is plotted as a function of time.

RESULTS AND DISCUSSION

Effect of Trajectory Banking Position on Vehicle Ranges

Basic lift scheme.- The effect of trajectory banking position (point on trajectory where banking is initiated) on the lateral and longitudinal ranges of the descending vehicle for the basic lift scheme (α constant at 25°) is shown in figure 4. A bank angle of 45° was applied and held for banking intervals of both 10° and 20°. Each position plotted is marked with the value of the trajectory position at which banking was initiated. The change in lateral range is plotted against the change in longitudinal range as measured at an altitude of 100,000 feet. For a banking interval of 10° (fig. 4(a)), maximum lateral range results when the banking maneuver is performed at trajectory positions in the region between $K = 345^\circ$ and 353°. When the banking interval ΔK is increased to 20° (fig. 4(b)), the region for maximum lateral range is between $K = 330^\circ$ and 340°.

The regions given not only define the maximum lateral range for a given banking interval, but also the region for obtaining lateral range with minimum loss in longitudinal range. This result is evident by the fact that the slope of the straight line connecting the origin with a data point is greatest in the region defined by maximum lateral range. For a value of $\Delta K = 10^\circ$, a maximum slope of 1.24 occurs at $K = 345^\circ$, and for $\Delta K = 20^\circ$, a maximum slope of 1.04 occurs at $K = 330^\circ$.

Figure 4 shows that the variation of ΔR_{long} is not regular with bank position. Calculations with a nonrotating spherical earth replacing the oblate rotating earth showed the same irregular variation of ΔR_{long} with bank position as shown in figure 4. These results indicate that this condition is caused by an interaction of the reentry vehicle and the atmosphere. Since the terms which give the short-period oscillation were not present in the equations of motion of the vehicle, it appears that this irregularity occurs during the period when a phugoid motion exists in the basic trajectory.

Optional lift scheme.- The effect of trajectory banking position on the lateral and longitudinal ranges of the descending vehicle for the optional lift scheme (α increasing during bank) is shown in figure 5. A bank angle of 45° and a banking interval of 10° were used. Range results presented compare unfavorably with results obtained with the basic lift scheme as evidenced by a comparison of figure 5 with figure 4(a). Not only is more lateral range obtained with the basic lift scheme (321 nautical miles as compared with 228 nautical miles), but also less longitudinal range is lost (265 nautical miles as compared with 830 nautical miles). Since the optional lift scheme did not compare favorably with the basic lift scheme, no further results were obtained by this method.

Effect of Bank Angle on Vehicle Ranges

The effect of bank angle on the lateral and longitudinal ranges of the vehicle was investigated for a range of banking positions. The results are presented in the following table for bank angles of 30°, 45°, and 60° at selected banking positions of 90°, 120°, 255°, 315°, and 345°:

K, deg	Case 1 $\phi = 30^\circ$, $\Delta K = 10^\circ$		Case 2 $\phi = 45^\circ$, $\Delta K = 10^\circ$		Case 3 $\phi = 60^\circ$, $\Delta K = 10^\circ$		Case 4 $\phi = 30^\circ$, $\Delta K = 20^\circ$	
	ΔR_{lat}, nautical miles	ΔR_{long}, nautical miles	ΔR_{lat}, nautical miles	ΔR_{long}, nautical miles	ΔR_{lat}, nautical miles	ΔR_{long}, nautical miles	ΔR_{lat}, nautical miles	ΔR_{long}, nautical miles
90	-0.3	-29	-0.5	-63	-0.7	-106	-0.9	-79
120	-1.9	-127	-3.0	-263	-4.2	-433	-5.1	-304
255	18.7	-78	28.6	-180	39.0	-328	56.6	-181
315	115.5	-75	193.9	-212	303.0	-486	255.3	-156
345	194.4	-87	314.9	-253	445.2	-615	393.4	-228

A constant angle of attack of 25° and banking intervals of 10° and 20° were used. Results using a 45° bank angle and a banking interval of 10° were previously shown (fig. 4(a)), but are included for purposes of comparison. These results show that in all cases the magnitude of the change in lateral range increases as K increases from 90° to 345°. An inspection of cases 1, 2, and 3 for values of K of 255°, 315°, and 345° shows that the change in lateral range increases as the bank angle is increased from 30° to 60°. However, it may also be noted that longitudinal-range losses are increased sharply as the bank angle is increased. For $K = 345^\circ$ and a bank angle of 30°, the change in lateral range is some 100 percent more than the loss in longitudinal range, but when the bank angle is increased to 60°, the increase in lateral range is some 30 percent less than the loss in longitudinal range.

The results for bank angles of 30° and 60° indicate that it may be more desirable as far as loss in longitudinal range is concerned to use a smaller bank angle and a longer banking interval to obtain some given lateral range. When cases 2 and 4 are compared for values of K of 315° and 345°, it is observed that not only is more lateral range obtained in case 4, but also less longitudinal range is lost.

Effect of Small Bank Angles and Long Banking Intervals on Vehicle Range

Some range results using small bank angles and rather large banking intervals were obtained and are presented in the table that follows for bank angles of 5°, 10°, and 15°. Banking intervals used are from K = 0°, K = 180°, and K = 270° to end of trajectory at 100,000-foot altitude.

K, deg	ϕ = 5°		ϕ = 10°		ϕ = 15°	
	ΔR_{lat}, nautical miles	ΔR_{long}, nautical miles	ΔR_{lat}, nautical miles	ΔR_{long}, nautical miles	ΔR_{lat}, nautical miles	ΔR_{long}, nautical miles
0	217	-78	427	-303	621	-675
180	219	-33	432	-169	629	-406
270	209	-8	410	-85	596	-231

Results show only small differences in lateral-range change for a given ϕ when the various banking intervals are compared. However, longitudinal-range losses are greatly affected by the choice of banking interval. The smallest longitudinal-range loss occurs for the shortest banking interval (K = 270°), and the greatest loss occurs for the longest banking interval (K = 0°). A comparison of the lateral-range and longitudinal-range changes for K = 270° in this table and the results of ϕ = 45° in figure 4 shows that lateral range may be obtained with less loss of longitudinal range if the smaller bank-angle scheme of the table is used. It is also interesting to note from this table that for a given banking interval the lateral-range change is approximately proportional to the bank angle, whereas the longitudinal-range change is not.

CONCLUDING REMARKS

An investigation has been made to determine the effects of banking position, bank angle, and banking interval on the lateral and longitudinal ranges of a hypersonic reentry glider of global-range capability. Results indicated that banking the vehicle during the first half of a global-range reentry results in relatively large losses of longitudinal range without any appreciable gain in lateral range. In addition, it was found that lateral range could be obtained

with less loss of longitudinal range if the scheme of using a small bank angle and an extended banking interval were used. An optional lift scheme which was used and which stabilized the vertical lift force during banking was not found to be as satisfactory as the basic lift scheme because of relatively large losses of longitudinal range and reduced lateral-range capability.

Langley Research Center,
National Aeronautics and Space Administration,
Langley Station, Hampton, Va., December 12, 1962.

APPENDIX A

EQUATIONS OF MOTION

The equations of motion of the vehicle in basic inertial spherical earth coordinates are

$$\ddot{L}_{c,i} = \frac{a_x}{r_i} - \frac{2\dot{h}\dot{L}_{c,i}}{r_i} + \dot{\eta}_i^2 \cos L_{c,i} \sin L_{c,i}$$

$$\ddot{\eta}_i = -\frac{a_y}{r_i \sin L_{c,i}} - \frac{2\dot{h}\dot{\eta}_i}{r_i} - 2\dot{L}_{c,i}\dot{\eta}_i \frac{\cos L_{c,i}}{\sin L_{c,i}}$$

$$\ddot{h} = -a_z + r_i\dot{L}_{c,i}^2 + r_i\dot{\eta}_i^2 \sin^2 L_{c,i} - \frac{g_e r_e^2}{r_i^2}$$

where a_x, a_y, and a_z are component accelerations in the x, y, and z directions, respectively, which result from oblateness and aerodynamic forces. These accelerations may be written in the form

$$a_x = a_{x,ob} + a_{x,a}$$

$$a_y = a_{y,ob} + a_{y,a}$$

$$a_z = a_{z,ob} + a_{z,a}$$

where the subscripts ob and a denote acceleration components due to oblateness and aerodynamic forces. These components are defined as follows:

$$a_{x,ob} = 6\mu g_e \frac{r_e^4}{r_i^4} \sin 2L_{c,i}$$

$$a_{y,ob} = 0$$

$$a_{z,ob} = -3\mu g_e \frac{r_e^4}{r_i^4}\left(1 + 3 \cos 2L_{c,i}\right)$$

$$a_{x,a} = -\frac{D}{m}\cos\psi\cos\theta - \frac{L}{m}\cos\psi\sin\theta\cos\phi - \frac{L}{m}\sin\psi\sin\phi$$

$$a_{y,a} = -\frac{D}{m}\sin\psi\cos\theta - \frac{L}{m}\sin\psi\sin\theta\cos\phi + \frac{L}{m}\cos\psi\sin\phi$$

$$a_{z,a} = \frac{D}{m}\sin\theta - \frac{L}{m}\cos\theta\cos\phi$$

The $a_{x,a}$, $a_{y,a}$, and $a_{z,a}$ acceleration components were determined from the aerodynamic force equations in stability axes

$$\bar{L} = -L\bar{k}_s$$

$$\bar{D} = -D\bar{i}_s$$

and the vector transformation between the X, Y, Z and X_s, Y_s, Z_s axes system is

$$\begin{bmatrix} \bar{i} \\ \bar{j} \\ \bar{k} \end{bmatrix} = \begin{bmatrix} \cos\psi\cos\theta & \cos\psi\sin\theta\sin\phi - \sin\psi\cos\phi & \cos\psi\sin\theta\cos\phi + \sin\psi\sin\phi \\ \sin\psi\cos\theta & \sin\psi\sin\theta\sin\phi + \cos\psi\cos\phi & \sin\psi\sin\theta\cos\phi - \cos\psi\sin\phi \\ -\sin\theta & \cos\theta\sin\phi & \cos\phi\cos\theta \end{bmatrix} \begin{bmatrix} \bar{i}_s \\ \bar{j}_s \\ \bar{k}_s \end{bmatrix}$$

The velocity components of the vehicle in the x, y, z directions with respect to the rotating earth are

$$V_x = r_i\dot{L}_{c,i}$$

$$V_y = -r_i\dot{\lambda}\sin L_{c,i}$$

$$V_z = -\dot{h}$$

where

$$\dot{\lambda} = \dot{\eta}_i - \omega$$

These components are used to compute the following:

$$V_e^2 = V_x^2 + V_y^2 + V_z^2$$

$$q = \frac{\rho}{2} V_e^2$$

$$L = qSC_L(\alpha,M)$$

$$D = qSC_D(\alpha,M)$$

$$\psi = \tan^{-1} \frac{V_y}{V_x}$$

$$\theta = \sin^{-1} - \frac{V_z}{V_e}$$

The atmospheric density is a function of local altitude h_e and is based on the 1959 ARDC model atmosphere (ref. 2). Local altitude h_e is defined by the equation

$$h_e = h + 70,459 \cos^2 L_{c,i}$$

where h is

$$h = h_0 + \int_0^t \dot{h}\, dt$$

The magnitude of the radius vector is

$$r_i = r_e + h$$

where r_e is the equatorial radius of the earth.

APPENDIX B

DERIVATION OF CONVERSION EQUATIONS

The position of the vehicle in the x_i, y_i, z_i and x_r, y_r, z_r inertial coordinate systems in spherical coordinates are as follow:

$$x_i = r_i \sin L_{c,i} \cos \eta_i$$

$$y_i = r_i \sin L_{c,i} \sin \eta_i$$

$$z_i = r_i \cos L_{c,i}$$

$$x_r = r_r \sin L_{c,r} \cos \eta_r$$

$$y_r = r_r \sin L_{c,r} \sin \eta_r$$

$$z_r = r_r \cos L_{c,r}$$

The transformation between the two inertial coordinate systems in matrix form is

$$\begin{bmatrix} \bar{i}_r \\ \bar{j}_r \\ \bar{k}_r \end{bmatrix} = \begin{bmatrix} 1 & 0 & 0 \\ 0 & \cos \sigma & \sin \sigma \\ 0 & -\sin \sigma & \cos \sigma \end{bmatrix} \begin{bmatrix} \bar{i}_i \\ \bar{j}_i \\ \bar{k}_i \end{bmatrix}$$

where $\bar{i}_r$, $\bar{j}_r$, $\bar{k}_r$ and $\bar{i}_i$, $\bar{j}_i$, $\bar{k}_i$ are unit vectors in the x_r, y_r, z_r and x_i, y_i, z_i directions, respectively. The angle σ is the transformation angle. Use of these vector and scalar relationships and noting that $r_i = r_r$ yields the following equations:

$$\sin L_{c,r} \cos \eta_r = \sin L_{c,i} \cos \eta_i$$

$$\sin L_{c,r} \sin \eta_r = \cos \sigma \sin L_{c,i} \sin \eta_i + \sin \sigma \cos L_{c,i}$$

$$\cos L_{c,r} = -\sin \sigma \sin L_{c,i} \sin \eta_i + \cos \sigma \cos L_{c,i}$$

These relations are used in defining the conversion equations

$$\cos L_{c,r} = -\sin \eta_i \sin L_{c,i} \sin \eta_i + \cos \sigma \cos L_{c,i}$$

$$\tan \eta_r = \frac{\cos \sigma \sin L_{c,i} \sin \eta_i + \sin \sigma \cos L_{c,i}}{\sin L_{c,i} \cos \eta_i}$$

REFERENCES

1. Young, John W.: A Method for Longitudinal and Lateral Range Control for a High-Drag Low-Lift Vehicle Entering the Atmosphere of a Rotating Earth. NASA TN D-954, 1961.

2. Minzner, R. A., Champion, K. S. W., and Pond, H. L.: The ARDC Model Atmosphere, 1959. Air Force Surveys in Geophysics No. 115 (AFCRC-TR-59-267), Air Force Cambridge Res. Center, Aug. 1959.

TABLE I

LIFT- AND DRAG-FORCE COEFFICIENTS

$$\begin{bmatrix} C_L = C_{L,0} + C_{L,1}\alpha + C_{L,2}\alpha^2 \\ C_D = C_{D,0} + C_{D,1}\alpha + C_{D,2}\alpha^2 \end{bmatrix}$$

M	$C_{L,0}$	$C_{L,1}$	$C_{L,2}$	$C_{D,0}$	$C_{D,1}$	$C_{D,2}$
4	-0.0983	1.1946	-0.00547	0.043	-0.1461	1.3953
6	-.0983	1.1946	-.00547	.043	-.1461	1.3953
8	-.098	1.10	.00	.0445	-.18	1.48
10	-.0967	1.017	.1368	.0457	-.2607	1.5704
12	-.0967	1.017	.1368	.0472	-.2950	1.672
15	-.0967	1.017	.1368	.0513	-.3295	1.778
20	-.101	.9454	.197	.04367	-.2894	1.636
26	-.101	.9454	.197	.0583	-.318	1.6798

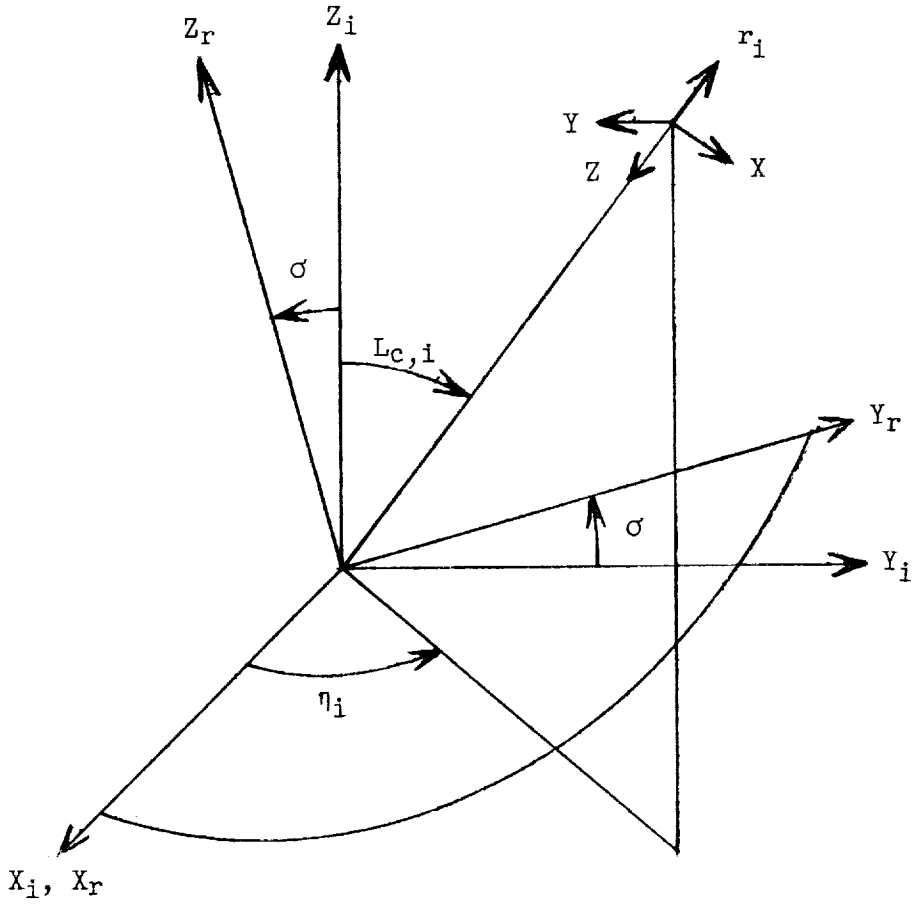

(a) Inertial-axes systems.

Figure 1.- Axes systems.

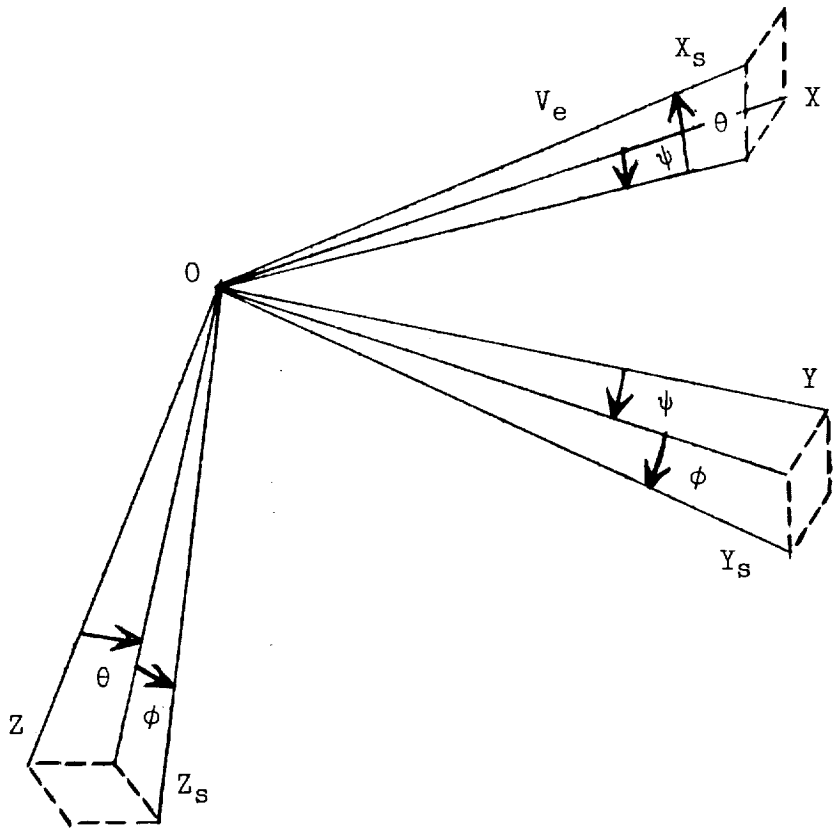

(b) Orientation of stability-axes system to reference axes system.

Figure 1.- Concluded.

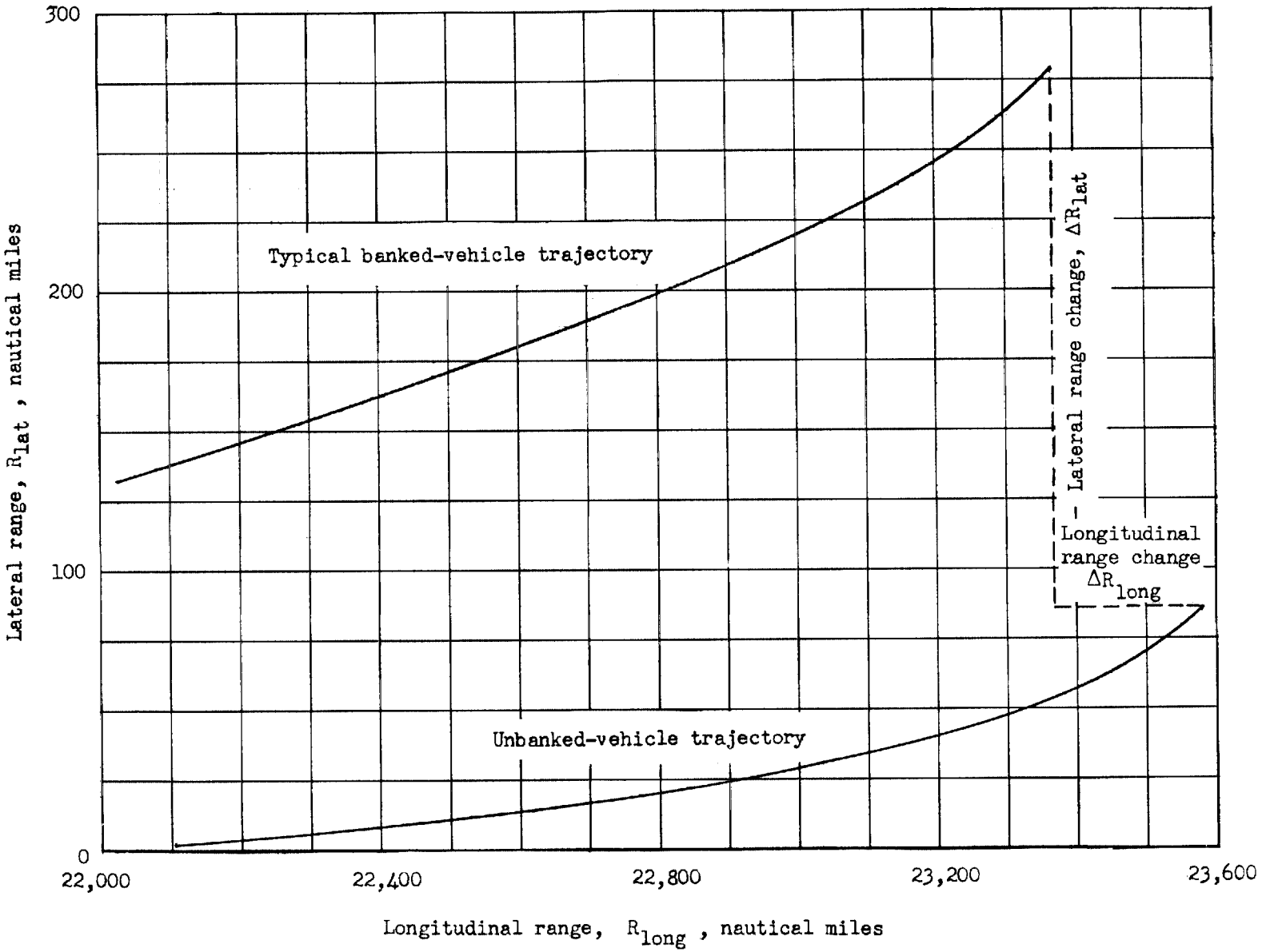

Figure 2.- Graphical illustration of how changes in lateral and longitudinal ranges are measured relative to range of unbanked-vehicle trajectory.

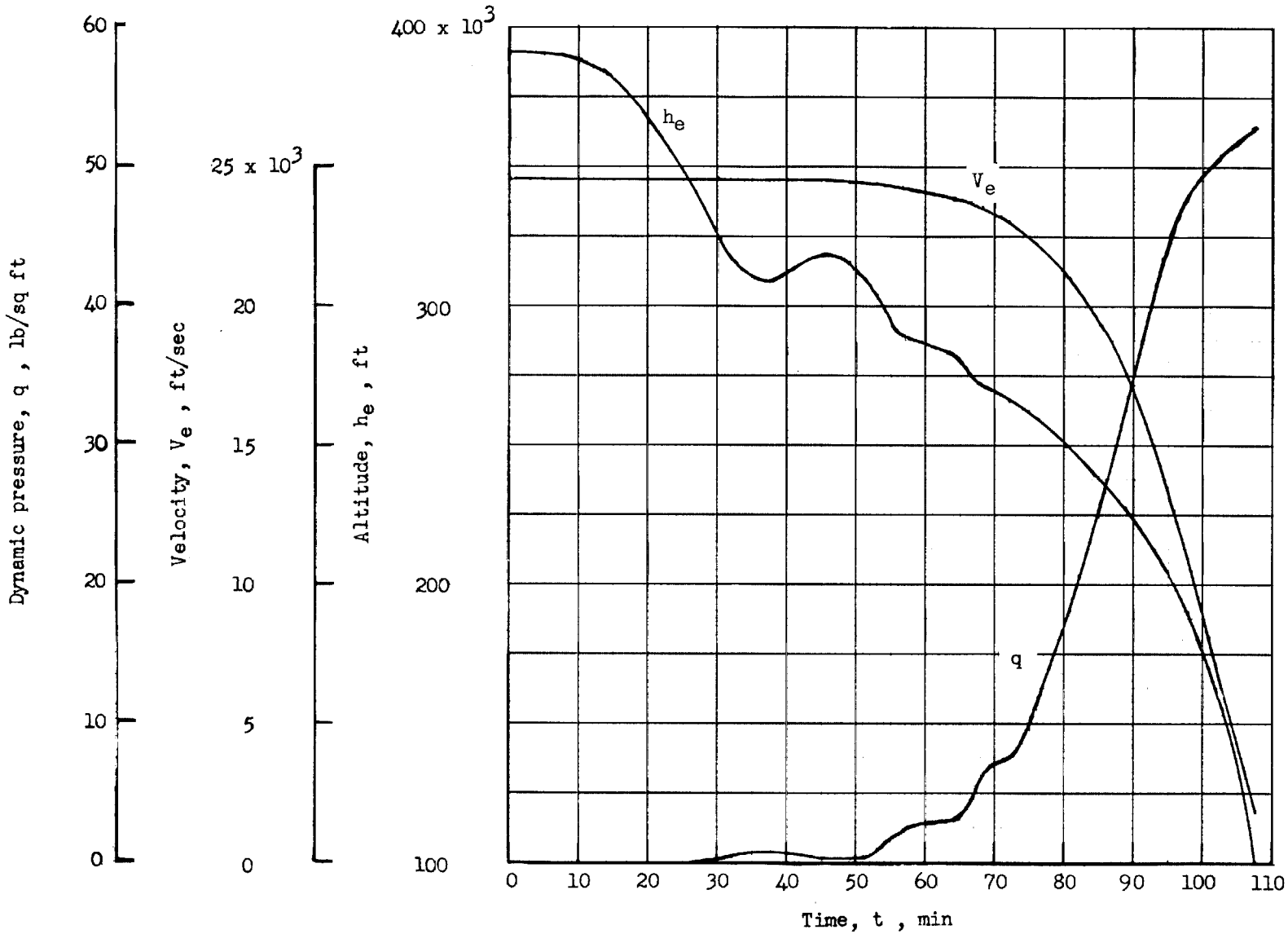

Figure 3.- Variation of dynamic pressure, velocity, and altitude with time for the unbanked reentry vehicle.

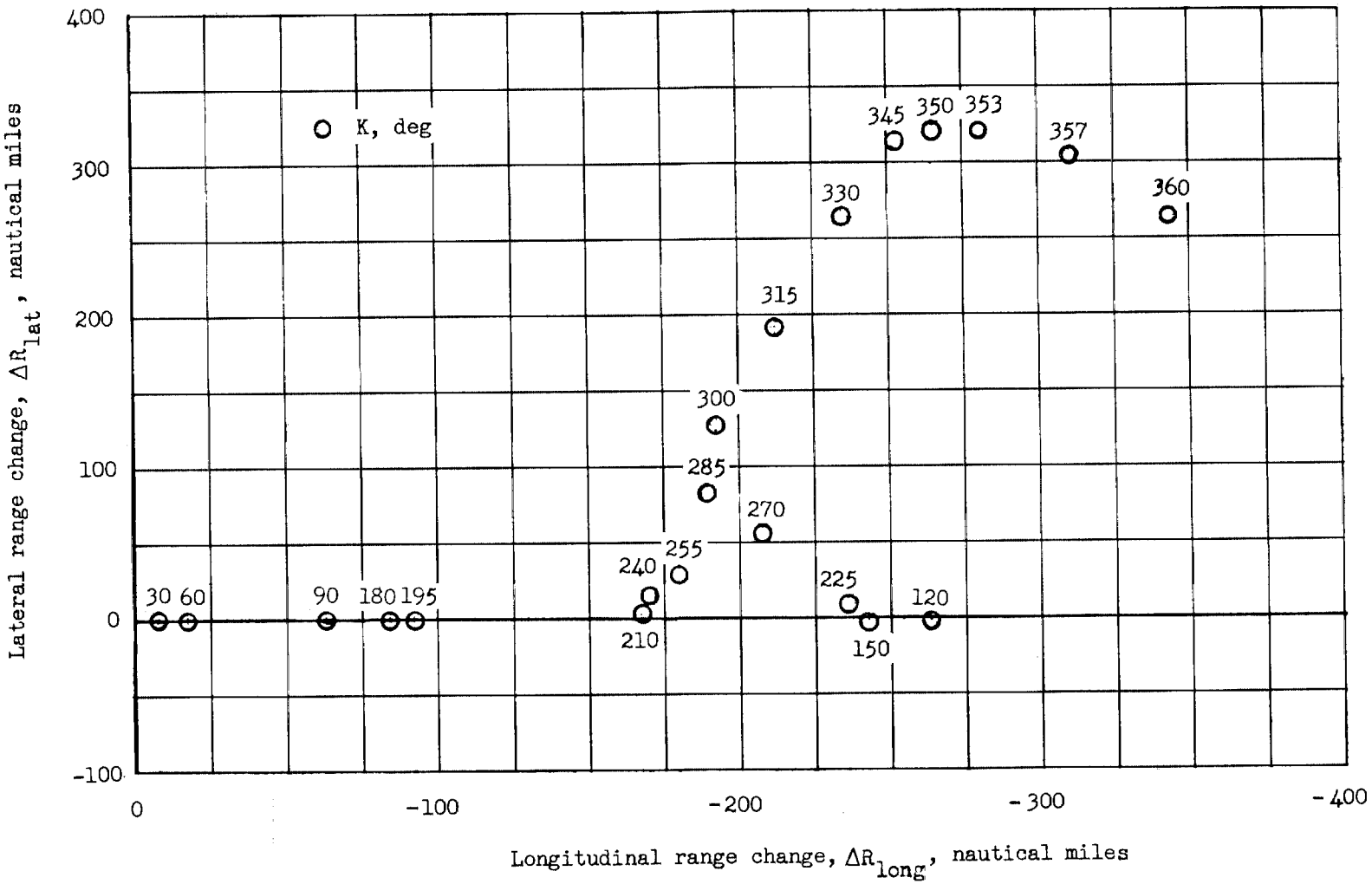

(a) $\Delta K = 10^{o}$.

Figure 4.- Effect of banking vehicle on lateral and longitudinal ranges at various trajectory positions and for a constant banking interval. Basic lift scheme; $\phi = 45^{o}$.

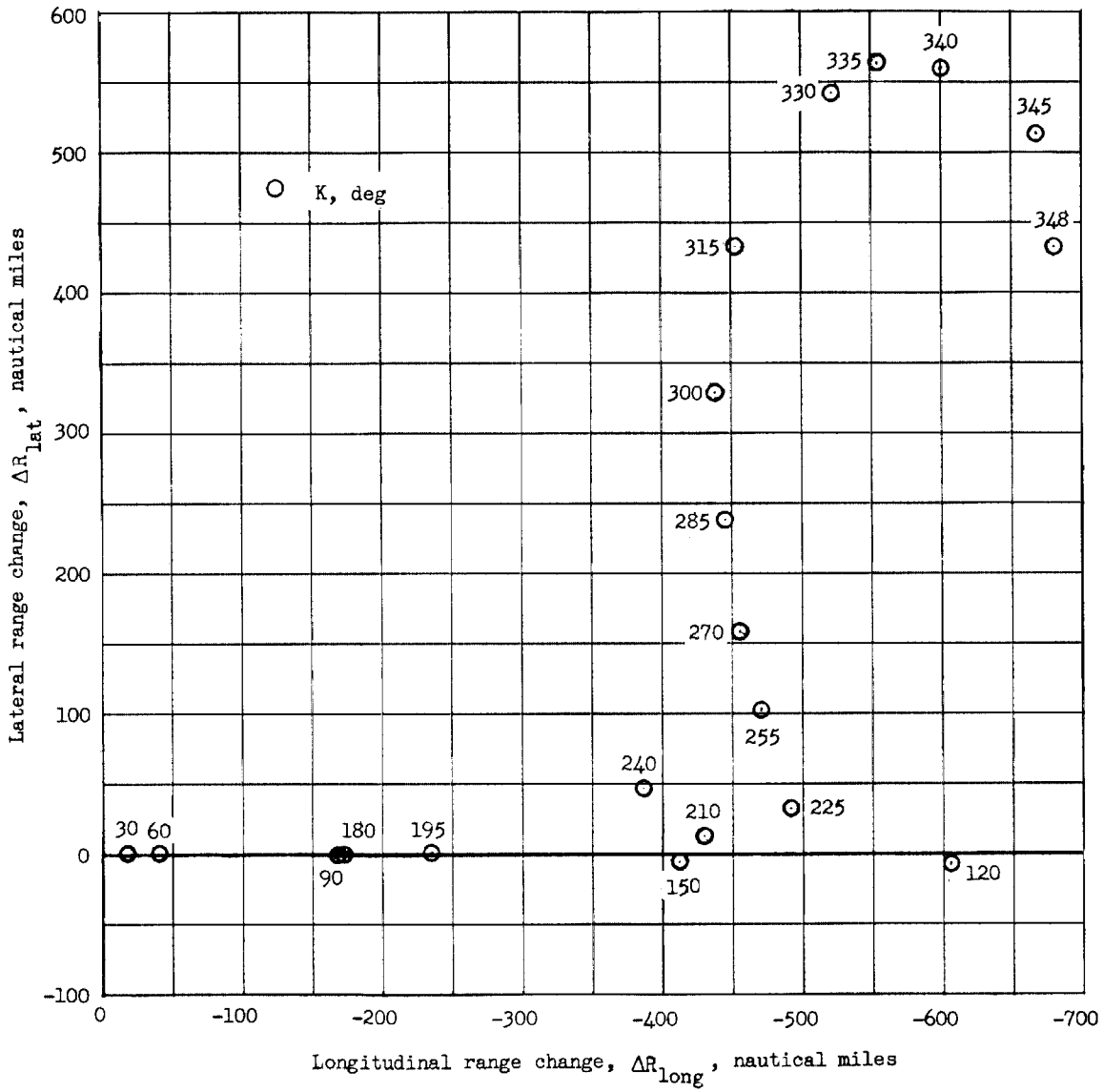

(b) $\Delta K = 20^{\circ}$.

Figure 4.- Concluded.

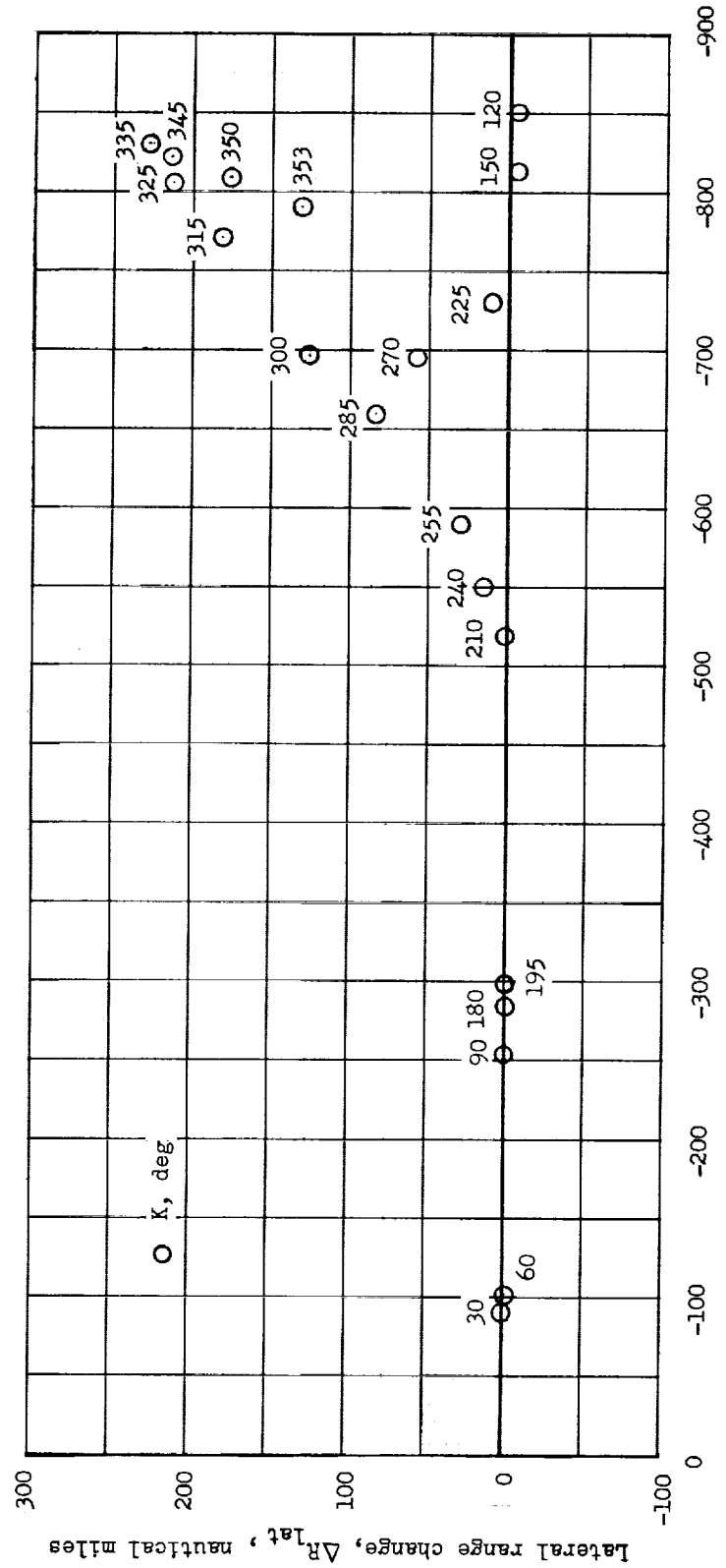

Figure 5.- Effect of banking vehicle on lateral and longitudinal ranges at various trajectory positions and for a constant banking interval. Optional lift scheme; $\phi = 45^{\circ}$; $\Delta K = 10^{\circ}$.

NASA-Langley, 1963 L-3159